Chapter 8
Ionospheric Threat Model Methodology for China Area

Dun Liu, Li Chen, Liang Chen and Weimin Zhen

Abstract The ionosphere is the largest remaining error source affecting GNSS regional augmentation system. The situation could be more serious when there is no enough measurement in a limited areas monitored by the network. The spatial threat model is constructed to restrict the ionospheric behavior under these under-sample scenarios for a more stringent bound. In this work two ionospheric spatial threat model, namely 'blob' and 'wall' models are constructed. In the 'blob' model, ionospheric delay increase with radius of 'blob' until the saturation is reached at a distance of 500 km. In the 'wall' model, ionospheric delay increase with the distance of ionospheric grids to 'wall'. Different ionospheric behavior during the storm for China area and North America area is responsible for the different model variation.

Keywords GNSS · Ionosphere · Integrity · Spatial threat model

8.1 Introduction

Ionospheric grid model is generally used for ionospheric delay correction and its error bounding in GNSS regional augmentation system. The essence of grid model is a planner fitting of ionospheric delays at fixed grid points with measured delays at ionospheric pierce points (IPPs). Spatial correlation model is used in the grid model to depict the spatial behavior of the ionospheric delays for effective error overbounding [1, 2, 3].

Based on its utilization, three kinds of ionospheric spatial correlation model could be made, namely zero-order spatial correlation model, first-order spatial correlation and spatial threat model. The zero and first order model is used to depict the ionospheric error and its residual characteristics of the planner fitting in

D. Liu (✉) · L. Chen · L. Chen · W. Zhen
No.22nd Research Institute, CETC, 266107 Qingdao, China
e-mail: dun.l@163.com

ionospheric grid model, while the spatial threat model is used to describe the effects caused by under-sampled ionospheric measurements to grid model.

Steep ionospheric delay gradient exists in ionospheric storms, degrading the grid model performance. The situation is more serious when there are no enough IPP measurements [4–7]. A spatial threat model is used to increase the GIVEs (Grid Ionospheric Vertical Error) to over-bound the ionospheric residuals.

In this paper the ionospheric spatial threat model methodology is presented. Two kinds of models namely "blob" and 'wall' spatial threat model are studied for China area. Comparison of models in China and North America area is made also.

8.2 Data and Preprocessing in Model Construction

8.2.1 Data Used in Model Construction

Data used in the spatial thread model construction includes:

(1) GPS dual-frequency measurements
    GPS dual-frequency data from stations (Fig. 8.1) in and around China areas are used to retrieve ionospheric delay.
(2) Solar terrestrial space environment data
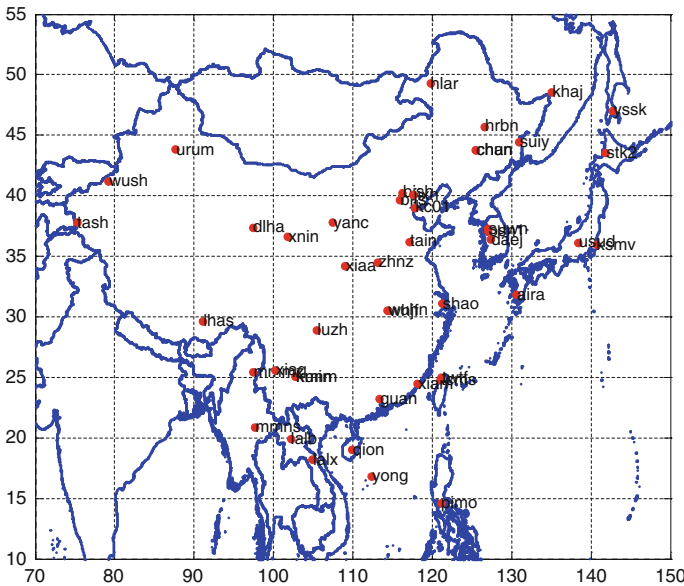   The data such as Kp index are used for judgment of ionospheric disturbance.

Fig. 8.1 GPS network in China and around area

8.2.2 Pre-process of GPS Data

The following procedure is used to retrieve ionospheric delay precisely.

 (a) Ionospheric delay is calculated with the carrier phase smoothed pseudo-range measurements.
 (b) DCB (Differential code bias) of GPS satellites from CODE (Center for Orbit Determination in Europe) is used.
 (c) GPS receiver hardware bias is estimated with data before and after stormy days and averaged to improve the accuracy. Comparison with IGS published data shows an accuracy of better than 0.5 ns.

With these data ionospheric delays are retrieved in stormy days for modeling.

8.3 Ionospheric Spatial Threat Model Construction

Two kinds of spatial threat model are constructed, namely the 'blob' model and the 'wall' model.

8.3.1 'Blob' Spatial Threat Model

When unevenly distributed IPPs measurements are used to estimate ionospheric delays on grids, there may be the possibility that an un-sampled area exists leading to errors in the estimation. Figure 8.2 is a schematic drawing for "blob" model.

In the modeling of this scenario, a region of 'blob' can be formed by removing IPPs stepwise. Then the ionospheric delay at the grid point is estimated with the measurements at the remaining pierce points. The estimated delays are compared with the real ionospheric delay at the grid point. With this method, residual variation of the estimated ionospheric delays at the grid point with the extension of the 'blob' region can then be studied, consequently with 'blob' spatial threat model constructed.

Figures 8.3 and 8.4 shows the result of the 'blob' spatial threat model with GPS data of 2011/04/01 when a strong ionospheric storm occurred. Figure 8.3 is the histogram for ionospheric delay residual with 'blob' radius, while Fig. 8.4 is plot for statistical ionospheric delay residual with 'blob' radius. It can be seen that when the radius of the 'blob' is less than 250 km, ionospheric delay residual increase with the radius; when the radius is more than 500 km, little variation of the residual happens, i.e. saturation reached.

'Blob' spatial threat model shows that measurements within the distance of 250 km to the grid point have the most effects in the grid ionospheric delay estimation. As the distance increase, contribution to the ionospheric delay estimation at
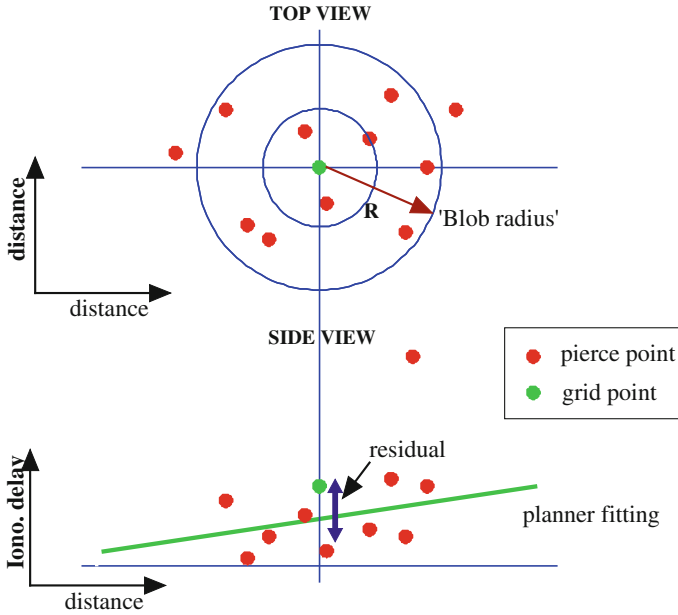
Fig. 8.2 Schematic drawing for 'blob' spatial threat model

the grid point decrease for measurements far from the grid. That is, as the distance increasing, only a rough ionospheric planar fitting can be made with the measurements far from the grid point, and variation of the ionospheric delay, especially the large gradient in the 'blob' cannot be detected.

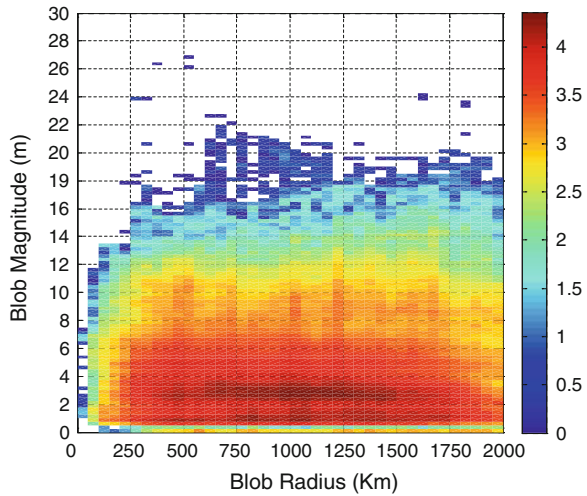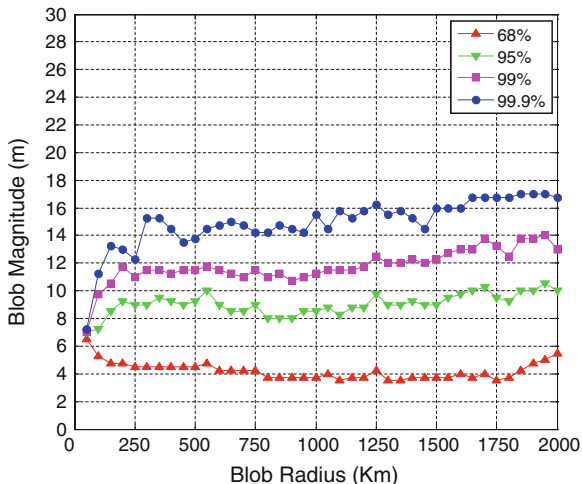**Fig. 8.3** Histogram for ionospheric delay variations with 'blob' radius

Fig. 8.4 Plot for ionospheric
delay statistical variations
with 'blob' radius

8.3.2 'Wall' Spatial Threat Model

In the 'wall' spatial threat model, ionospheric IPPs locate on the same side of the
grid point, large residual of the ionospheric delay at the grid point will be caused
with measurements at these IPPs. It describes an extreme scenario which occurs
often near the border of the regional augmentation system. Schematic drawing for
'wall' spatial threat model is shown in Fig. 8.5.

Fig. 8.5 Schematic drawing
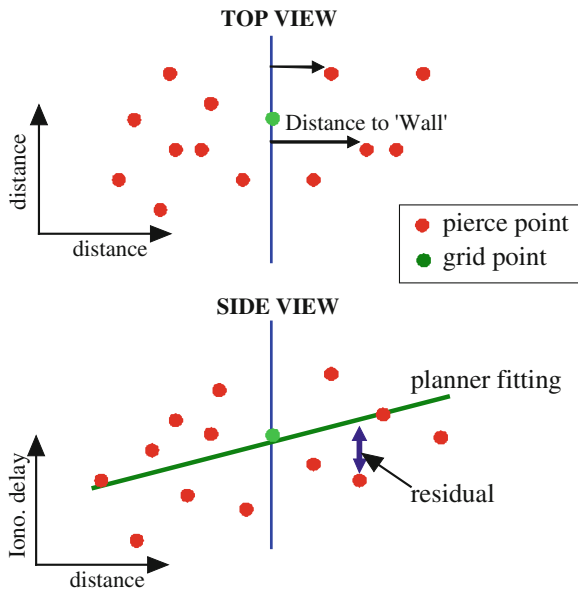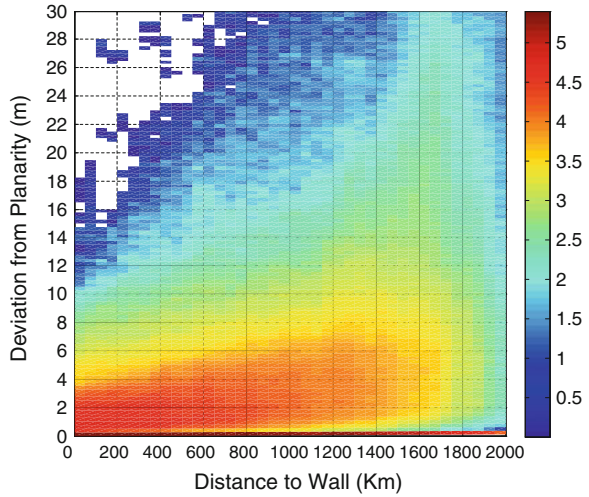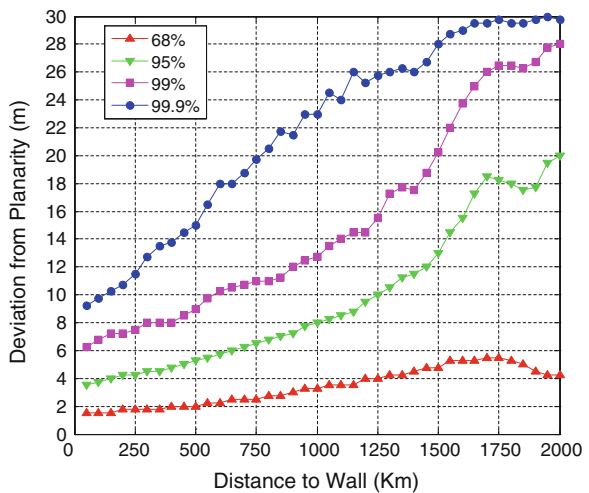for 'wall' spatial threat model

Fig. 8.6 Histogram for ionospheric delay variations with distance to the 'wall'

In the 'wall' spatial threat modeling, a region formed by removing pierce points on one side of the 'wall'. Then the ionospheric delay at the grid point can be estimated with the measurements at the remaining pierce points. The estimated delays are compared with the real ionospheric delay at the grid point. With this method, residual variation of the ionospheric delay at the grid point with the distance from the grid point to the 'wall' can be studied.

Figures 8.6 and 8.7 show the result of the 'wall' spatial threat model with GPS data of 2011/04/01. Figure 8.6 is histogram for ionospheric delay residual with distance to the 'wall', while Fig. 8.7 is plot for statistical ionospheric delay residual variations with distance to the 'wall'. It can be seen that residual of the ionospheric delay always increase with the distance from the grid points to 'wall'.

Fig. 8.7 Plot for ionospheric delay statistical variations with distance to the 'wall'

'Wall' spatial threat model shows that residual of the ionospheric delay increase with the distance from the 'wall' to the grid point. The measurements at the pierce points used for grid ionospheric delay estimation cannot describe the overall spatial variation of the ionosphere since they are all located at one side of the grid point. When the grid model is constructed with the measurements at one side of the 'wall' and extended to the area on the other side, large error arise as only information on one side of the 'wall' could be used.

8.4 Comparison of Ionospheric Threat Model in China and North America Areas

Spatial threat model in China area and that in North America are compared to show their characteristics [5–7].

Significant difference exists in two 'blob' spatial threat models. In China area residual of the ionospheric delay increase with the radius less than 250 km, and saturation is reached when the radius of the 'blob' is more than 500 km. While in North America, residual of the ionospheric delay increases always with increase of the radius [7].
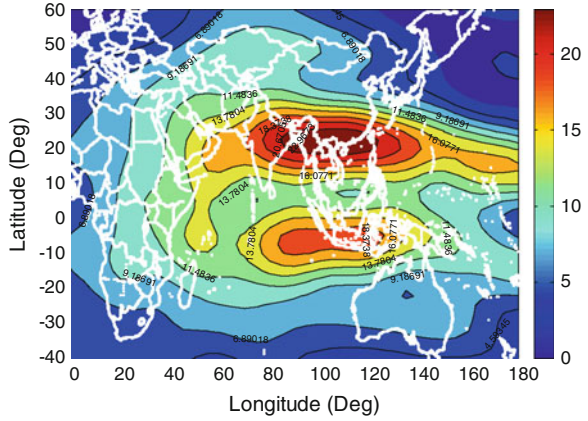
No much difference exists in two 'wall' spatial threat model. For the model in North America areas given by Raytheon Corp, residual of the ionospheric delay varies mild when the distance is small, but increase abruptly when the distance is large [7]. For China areas, residual varies mild when the distance is less than 500 km, but increase fast when the distance is more than 500 km (see the 1σ ionospheric delay residual variation). This trend is more evident for the 2σ ionospheric delay residual.

Difference in the spatial threat model in China and North America is analyzed with GIM TEC map. Figures 8.8 and 8.9 shows the typical variation of ionospheric delay respectively in these two regions during the ionospheric storm occurred at 2003/10/29.

During the storm, gradient of ionospheric delay extended from south-east to north-west in North America. That is, big gradient occurs in a narrow and small region while in other part the ionospheric delay varies mild. Similar characteristics also be found in other storm events in years of 2000–2003. This characteristic of gradient variation in the ionospheric delays makes the error in the planar fitting with IPPs ionospheric delays increase as the 'blob' radius increase or the number of IPPs use for grid delay estimation decrease.

For China region steep gradient existed from south to north while small variation existed from east to west in the ionospheric delays during storm. The gradient lies between the belt with the maximum ionospheric delays where Guangzhou, Hainan and Kunming locate and the belt of mild ionospheric delays where Shanghai, Wuhan and Chongqing locate.

Fig. 8.8 Ionospheric delay
distribution during the storm
of 29th October 2003 for
China area

Fig. 8.9 Ionospheric delay
distribution during the storm
of 29th October 2003 for
North America area

The gradient of ionospheric delay in the south-north direction has great effect to
the 'blob' model while that along the east-west direction contribute little. When the
'blob' radius is less than the distance of the steep gradient variation from south to
north (about 500 km), the ionospheric delay error increases fast with the increasing
of the radius of the 'blob'. When the radius is larger than that distance, the iono-
spheric delay errors reach the maximum, i.e. the saturation state reached.

China region covers the low and mid latitude areas, in which complicated ion-
ospheric delays variation happen during storms. The situation is even more com-
plicated with the effects of ionospheric anomaly superposed. The North America
locates in mid latitude region, large ionospheric delays gradients are caused mainly
by storms extended from the low latitude areas. Different characteristics the iono-
spheric storms in these two regions are responsible for the difference of the spatial
threat models.

8.5 Conclusion

Under-sampled observations in GNSS regional augmentation system will cause large error in the ionospheric grid model and failure of integrity. The condition becomes much more serious when ionospheric storms happen. The ionospheric spatial threat model is constructed to set up a more stringent bound of the ionospheric delay residuals.

Two type of spatial threat models namely the 'blob' model and the 'wall' model are studied and constructed with GNSS data during the ionospheric storm in China region. 'Blob' model shows an increasing ionospheric delay residual with the 'blob' radius until saturation state reached at the distance about 500 km. In the 'wall' model the ionospheric delay residual increases with the distance to the wall monotonously.

The spatial threat model for China areas and North America areas shows difference which is caused by the different characteristics of ionospheric delays during ionospheric storms in these two regions.

References

1. Hansen A, Peterson E, Walter T, Enge P (2000) Correlation structure of ionospheric estimation and correction for WAAS. In: ION NTM 2000, pp 454–463
2. Hansen A, Walter T, Blanch J, Enge P (2000) Ionospheric spatial and temporal correlation analysis for WAAS: quiet and stormy. In: ION GPS 2000, pp 634–642
3. Liu D, Zhen W, Chen L (2013) Ionospheric spatial correlation analysis for China area, In: CSNC, Guangzhou
4. Walter T, Hansen A, Blanch J, Enge P et al (2000) Robust detection of ionospheric irregularities. In: ION GPS 2000, pp 209–218
5. Blanch J, Walter T, Enge P (2002) Ionospheric threat model methodology for waas. Navigation 49(2):103–107
6. Blanch Juan, Walter Todd (2001) Per Enge. Ionospheric threat model methodology for WAAS, ION AM
7. Altshuler ES, Robert M (2001) Fries and Lawrence sparks, The WAAS ionospheric spatial threat model. In: ION GPS 2001, pp 2463–2467
8. Liu D, Zhen W (2012) The effects of china regional ionosphere on satellite augmentation system. Chin J Radio Sci 27(1):195–203